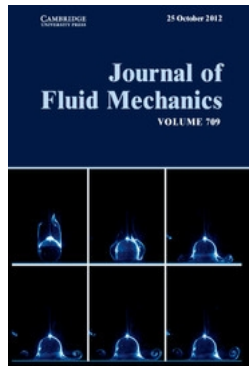

Short-scale effects on model boundary-layer spots

R. G. A. Bowles and F. T. Smith

Journal of Fluid Mechanics / Volume 295 / July 1995, pp 395 - 407
DOI: 10.1017/S0022112095002023, Published online: 26 April 2006

J. Fluid Mech. (1995), *vol.* 295, *pp.* 395–407

Short-scale effects on model boundary-layer spots

By R. G. A. BOWLES[1] AND F. T. SMITH[2]

[1]School of Mathematics and Statistics, University of Middlesex, London N11 2NQ, UK

[2]Department of Mathematics, University College London, London WC1E 6BT, UK

(Received 9 May 1994 and in revised form 7 April 1995)

This theoretical work, on the spot in an otherwise laminar boundary layer, concerns the initial-value problem for three-dimensional inviscid disturbances covering a wide range of scales. The study asks whether or not comparatively short scales can have a substantial impact on the spot spreading rate, as well as on other important features including the spot structure. It is found that such scales act to reduce the spread angle to approximately 11°, close to the experimental observations for transitional/turbulent spots, as opposed to the angle of 19.47° for waves near or behind the spot trailing edge. The scales emerge from coupling uniform shear flow directly with the local uniform stream and then analysing large-time features. The leading edge and trailing edge of the spot are also examined in detail, along with other structural properties. It is concluded that nonlinearity and short-scale effects probably combine to restrict the global spread angle as above, while viscous sublayer bursting among other things completes the spot structure. Related work on nonlinear, trailing-edge and leading-edge behaviours and comparisons with experiments are also discussed.

1. Introduction

The unsteady 'spot' is a patch of disturbed fluid travelling in an otherwise undisturbed flow, such as a boundary-layer or channel flow. The name was coined by Emmons (1951) who was the first to investigate this phenomenon. The flow within the spot may be laminar, transitional or turbulent. It is this last case which has been the main focus of the numerous experimental and computational studies on spots. The flow within turbulent spots exhibits features seen in structures within fully turbulent flows, as shown, for example, by Glezer, Katz & Wygnanski (1989), and it is therefore felt that an understanding of such spots may lead to greater insight into turbulence itself. As well as furthering this ultimate aim, however, a knowledge of spots is already used, by aerospace companies such as Rolls Royce for example, to predict and model transition to turbulence, providing an estimate for the intermittency factor in transitional flows. Experimentally, spots in both boundary-layer and plane Poiseuille flows are generated by artificial means, usually by an acoustic pulse or a spark, and the evolution of the spot is closely monitored. It is known (see Elder 1960) that a spot may be generated very rapidly, even at subcritical Reynolds numbers, by a sufficiently strong initial disturbance, bypassing the well-known natural routes to transition.

The gross characteristics of the spot, i.e. the 'arrowhead' shape and 'overhanging' front, the 'calm region' behind the main body of the spot, the lateral and

streamwise spreading rates and the speed of travel downstream are therefore well-documented: see for example Glezer *et al.* (1989) and references therein. Further intriguing features are also revealed by experiments, such as the maximum height of the spot occurring near the centre of the plan view, and the maximum turbulent intensities being at the peripheries of the spot rather than at the core. Wave-packets are seen to trail the spot. The linear theoretical works of Gaster (1968) and Doorly & Smith (1992) consider the development of a three-dimensional wave-packet at super-critical Reynolds numbers and show the formation of a caustic that limits the spread of such waves. The experiments of Katz, Seifert & Wygnanski (1990) with flows at subcritical Reynolds numbers indicate that in this regime the packets are simply 'passive attendants', suggesting that the spread and growth of the spot is not due only to these wave-packets but is achieved by strongly nonlinear processes in the spot itself.

Numerical three-dimensional unsteady simulations of transitional and turbulent spots tend to confirm the experimental findings: see, for example, Henningson, Lundbladh & Johnson (1993) and references therein. The generation of streamwise 'streaks', with reduced spanwise lengthscales, is a particularly interesting feature of these numerical spots, which also suggest that transition begins by a rapid growth in the normal velocity 'lifting up' low-speed fluid from near the wall.

The above wealth of qualitative and quantitative information about spots clearly raises many fascinating theoretical questions. It is equally clear that the phenomena involved are so complex that analytical progress can probably be made only by building up gradually from the relatively simpler laminar and transitional cases. In comparison with the progress made experimentally and numerically the theoretical work is as yet in its infancy, but an overall approach is suggested by Smith, Dodia & Bowles (1994) who consider the spot evolution as an initial-value problem, with different degrees of amplitude dependence. There are certain assumptions necessary, concerning initial conditions and amplitudes, but the main interest is in an increased understanding of the large-amplitude structure, which seems to fit together. The aim is to develop a rational model for the benefit of both fundamental understanding and the technological application described earlier, with its interest in pressure-gradient effects, spot spreading rates, spot production rates and collisions, among other properties.

The linear work of Doorly & Smith (1992) considers both incompressible and compressible boundary-layer flows and presents a large-time analysis. This shows the existence of two significant regions within the spot, at distances downstream proportional to $(\text{time})^{1/2}$ and (time). A feature of concern to the present paper is that the work of Doorly & Smith (1992) predicts the spread angle of the spot to be $\sin^{-1}(1/3)(\approx 19.47°)$. This is not in good agreement with experimental observations of the spread angle, which give an estimate closer to 11°, a matter taken up later in this section and in §3. The linear theory predicts that the maximum amplitudes within the spot occur at the edges or wingtips of the spot, in agreement with experimental results (see the second paragraph above). Nonlinearity would therefore be expected to become significant first in these regions and this development is examined by Smith (1992). The effects are shown to be confined to edge layers at the wingtips and arise from an interaction between the main fluctuations and the mean-flow correction. At increased input amplitudes the analysis points to a spreading of nonlinearity towards the centre of the spot. Dodia, Bowles & Smith (1995) present a study of a second edge layer astride the first which then contains the nonlinearity, again involving the interaction between the dominant fluctuations and the mean-flow correction. Again the effect of increased input amplitudes is to extend the region of

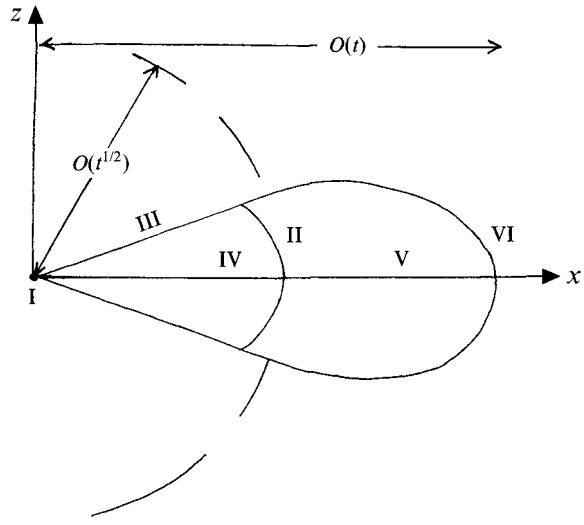

FIGURE 1. The various regions of the theoretical spot at large times t: I, the linear trailing edge; II, the nonlinear trailing edge; III, the edge layers; IV, the 'calm' region; V, the (nonlinear) centre; VI, the front.

nonlinear effects, which then eventually covers the whole spot. The latter becomes strongly nonlinear, the mean flow itself being significantly altered. Work on the flow solution in this region is currently under way.

Figure 1 presents an overview of the various regions. Behind the main body of the spot is the so-called 'calm' region. The flow within this region is observed experimentally to be *more* stable than the undisturbed flow: the displacement thickness of the boundary layer can be reduced in this region by a factor of just over a half (see Katz *et al.* 1990). Theoretically this region fits in as the centre of the spot before the nonlinearity floods inwards. It is discussed in Dodia *et al.* (1995). The front, or leading edge, of the spot is known to protrude downstream, overhanging relatively undisturbed fluid closer to the wall. The description of this region may be approached analytically by using the work of Smith, Doorly & Rothmayer (1990), who show the existence of high-vorticity regions, lying just outside the boundary layer, which move with a speed close to that of the free stream, as do the fronts of the spots observed experimentally.

The work presented here considers an alternative simple linear model, which, unlike the thin-layer work of Doorly & Smith (1992), crucially allows the existence of finite-wavelength modes. The lengths here are nondimensionalised with respect to the boundary-layer thickness. The spot may be thought of as a dispersion of these predominantly inviscid waves, the shorter waves generally forming the front while the trailing edge is made up of the longer, slower waves near the wall. On taking the long-wave limit we recover the long-wave results of Doorly & Smith (1992), while the presence of the finite wavelengths is found to produce a predicted spread angle remarkably close to the experimentally observed 11°. Here the spread angle is taken to be the angle between the free-stream direction and the direction to the maximum spot width, measured from the position of the initial disturbance. The main simplification in this model lies in the original two-dimensional boundary-layer profile (supporting linear or nonlinear small-amplitude disturbances), which is taken to be a simple shear beneath a uniform stream. This is perhaps the most obvious simple model to assume,

for a boundary-layer flow, and it allows considerable analytical progress to be made, giving the entire pressure field throughout the spot, cf. Doorly & Smith (1992). The predicted internal structure here is also in encouraging agreement with experiments. Further, the shape and structure of the leading edge, which is of particular interest, is examined in some detail. Altogether, although the above close agreement may be fortuitous, it is hoped that such a simple model may suggest guidelines for the investigation of the general nonlinear initial-value problem described above, given that in the general case, with a smooth initial profile, there may be no neutral linear waves but there are neutral nonlinear waves which may be considered analogously.

The unsteady three-dimensional Euler system is used below, for an incompressible boundary layer, as previous work (see for example Smith *et al.* 1990; Smith & Burggraf 1985; and Kachanov, Ryzhov & Smith 1993) indicates that this system can be the most appropriate for later or bypass stages of transition, allowing a *wide* band of $O(1)$ wavelengths, speeds and amplitudes for the initial disturbance, based on the displacement thickness and the free-stream speed. Viscous Tollmien-Schlichting (T-S) disturbances, by the way, are all generally smaller and slower by an order of magnitude. The lengthscales for the development of the present disturbance in the streamwise, normal and spanwise directions are all $O(Re^{-1/2})$, i.e. the Rayleigh scale, where Re is the global Reynolds number which is assumed to be large. Thus the coordinates scaling is equal in all three directions, unlike the 'thin-layer' system of T-S waves. The timescale, based on the free-stream speed and airfoil chord, is also $O(Re^{-1/2})$, faster than the T-S timescale.

In §2 the formulation of the model problem is presented and an integral solution for the pressure field is obtained. This expression is analysed in §3 for large times using the method of stationary phase. The resulting predicted position of the edge of the spot is discussed, including the 11° spread angle. In particular the position of the spot wingtip is examined in detail both at the trailing edge and at the leading edge, using asymptotic analysis. At the rear, the spread angle is shown to decrease from the long-wave 19.47° limit. The front in contrast is found to be nearly parabolic, for this model case, with the scaled spanwise coordinate of the wingtip, $z_w \sim \epsilon^{1/2}/(\ln 1/\epsilon)^{1/2}$, where ϵ is the scaled streamwise distance from the front and is assumed to be small. In §4 the numerical predictions for the pressure field and general spot features are presented and compared with experimental observations. These comparisons are encouraging, in qualitative or quantitative terms. The results and implications of this model problem are discussed further in §5. Whereas Smith (1992) and Dodia *et al.* (1995) show that nonlinear effects on their own tend to gradually reduce the spread angle, the present study indicates tentatively that the short-scaled content of the input disturbance may well be responsible for an even greater part of the reduction to 11° as found above; in reality both factors probably play significant roles in fixing the spread angle of nonlinear spots.

2. Formulation of model problem

As discussed in §1, the governing equations are the three-dimensional unsteady Euler equations. For the small disturbances of interest here the Euler equations may be linearized to give

$$u_t + Uu_x + vU_y = -p_x, \tag{2.1}$$

$$v_t + Uv_x = -p_y, \tag{2.2}$$

$$w_t + Uw_x = -p_z, \tag{2.3}$$

together with the equation of continuity. Here u, v, w are the nondimensional velocity components in the streamwise, normal and spanwise directions respectively, x, y, z are the corresponding nondimensional Cartesian coordinates, p is the nondimensional pressure and $U(y)$ is the background flow profile, given below. The boundary conditions and initial conditions are tangential flow at the wall, boundedness in the far field and a given initial pressure distribution.

We seek solutions $(u, v, w, p) = \mathrm{e}^{-\mathrm{i}\omega t}(\bar{u}, \bar{v}, \bar{w}, \bar{p})$, where ω is the wave frequency, and take a double Fourier transform in x, z, the transform variables being α and β, so that, for example,

$$u(x, y, z, t) = \frac{1}{4\pi^2} \int_{-\infty}^{\infty} \int_{-\infty}^{\infty} \hat{u}(\alpha, \beta, y) \mathrm{e}^{\mathrm{i}(\alpha x + \beta z - \omega t)} \mathrm{d}\alpha \, \mathrm{d}\beta. \tag{2.4}$$

We may eliminate p from the system thereby obtained from equations (2.1)–(2.3) and use the equation of continuity to find the effective Rayleigh equation for $\hat{v}$:

$$\hat{v}_{yy} - \hat{v}\left(\alpha^2 + \beta^2 + \frac{\alpha U_{yy}}{U\alpha - \omega}\right) = 0, \tag{2.5}$$

as expected. The boundary conditions give

$$\hat{v} = 0 \quad \text{at} \quad y = 0, \tag{2.6}$$

$$\hat{v} \to 0 \quad \text{as} \quad y \to \infty. \tag{2.7}$$

The background profile $U(y)$ is now defined in the present model case by

$$U(y) = \begin{cases} \lambda y & \text{for} \quad 0 \leqslant y \leqslant 1, \\ \lambda & \text{for} \quad y > 1. \end{cases}$$

The constant λ is to be taken as unity throughout this work, although a brief discussion of the effects of different values for λ and δ, the displacement thickness, is given later in §5. There is also a condition of continuity of pressure and vertical velocity necessary at $y = 1$,

$$\hat{v}, \hat{p} \quad \text{continuous} \quad \text{at} \quad y = 1, \tag{2.8}$$

associated with the presence of the shear discontinuity and corresponding thin sublayer there. In (2.8) $\hat{p}$ is given by

$$\hat{p} = \frac{\mathrm{i}}{\bar{\alpha}^2}(\alpha\hat{v} + (\omega - \alpha y)\hat{v}_y), \tag{2.9}$$

in terms of $\hat{v}$, from (2.1)–(2.3).

Equations (2.5)–(2.8) then yield the solution

$$\hat{v}(\alpha, \beta, y) = \begin{cases} \hat{A}\dfrac{\sinh \bar{\alpha} y}{\sinh \bar{\alpha}} & \text{in} \quad 0 \leqslant y \leqslant 1, \\ \hat{A}\mathrm{e}^{-\bar{\alpha}(y-1)} & \text{in} \quad y > 1, \end{cases} \tag{2.10}$$

for $\hat{v}$, together with the dispersion relation

$$\omega(\alpha, \beta) = \alpha - \frac{\alpha}{2\bar{\alpha}}(1 - \mathrm{e}^{-2\bar{\alpha}}), \tag{2.11}$$

where $\bar{\alpha}^2 = \alpha^2 + \beta^2$ and $\hat{A}$ is the transform of the initial vertical velocity at $y = 1$. From relation (2.11) it is clear that the shorter waves travel faster, with both the

phase speed ($\equiv \omega/\alpha$) and the group velocity ($\equiv \partial\omega/\partial\alpha$) tending to unity as $\bar{\alpha} \to \infty$; thus we may expect the front of the spot to consist mainly of such waves. In contrast, the trailing edge of the spot contains the longer slower waves with small phase speed and group velocity and indeed as $\bar{\alpha} \to 0$ we recover from (2.11) the thin-layer limit of Doorly & Smith (1992), i.e. $\omega = \alpha\bar{\alpha}$.

The entire pressure field may now be found by using equations (2.9) and (2.10), to give, on inversion,

$$p(x,y,z,t) = \frac{1}{4\pi^2}\int_{-\infty}^{\infty}\int_{-\infty}^{\infty} F(\alpha,\beta,y)\mathrm{e}^{\mathrm{i}(\alpha x+\beta z-\omega t)}\mathrm{d}\alpha\,\mathrm{d}\beta, \tag{2.12}$$

where

$$F(\alpha,\beta,y) = \begin{cases} \dfrac{\hat{Q}(\alpha,\beta)}{\bar{\alpha}\omega}(\bar{\alpha}(\omega-\alpha y)\cosh\bar{\alpha}y + \alpha\sinh\bar{\alpha}y) & \text{in} \quad 0 \leqslant y \leqslant 1, \\ \dfrac{\hat{Q}(\alpha,\beta)}{2\bar{\alpha}\omega}\alpha\sinh\bar{\alpha}(1-\mathrm{e}^{-2\bar{\alpha}})\mathrm{e}^{-\bar{\alpha}(y-1)} & \text{in} \quad y \geqslant 1. \end{cases} \tag{2.13}$$

Here $\hat{Q} = \mathrm{i}\hat{A}\omega/(\bar{\alpha}\sinh\bar{\alpha})$ is the transform of the initial pressure field at $y = 0$. The analysis below concentrates on this pressure distribution.

3. Large-time analysis and the spot shape

There is particular interest in both practical and theoretical terms in the spot response at relatively large times. The behaviour of the pressure disturbance at large t may be examined by using the method of stationary phase to analyse the integral in equation (2.12). We use polar coordinates R and θ in the plan view where θ is the angle from the free-stream direction and we consider comparatively large distances downstream of the initial disturbance such that $x = Rt\cos\theta$ and $z = Rt\sin\theta$. Similarly, we put $\alpha = r\cos\phi$ and $\beta = r\sin\phi$. Here α and β are $O(1)$. Other significant scales for x, z, α and β are discussed in §5. The phase function, from (2.11), $\psi(\equiv \alpha x/t + \beta z/t - \omega)$, then becomes

$$\psi(r,\phi) = rR\cos(\theta-\phi) + \tfrac{1}{2}(1-2r-\mathrm{e}^{-2r})\cos\phi. \tag{3.1}$$

We seek values for the pair (r,ϕ) such that

$$\psi_r = 0, \tag{3.2}$$

$$\psi_\phi = 0, \tag{3.3}$$

to provide the dominant contribution at large times. In practice this was carried out as follows. For given values of R, θ, substitution of (3.1) into (3.2) gives

$$\mathrm{e}^{-2r_0} = 1 - \frac{R\cos(\theta-\phi)}{\cos\phi}, \tag{3.4}$$

where $r_0(\phi)$ is the required root for r. Using this expression for $r_0(\phi)$, (3.3) becomes

$$\frac{\partial\psi(r_0,\phi)}{\partial\phi} = 0, \tag{3.5}$$

which gives an equation for ϕ_0,

$$\psi(r_0,\phi_0)\tan\phi_0 = \frac{r_0 R\sin\theta}{\cos\phi_0}. \tag{3.6}$$

The two values of ϕ_0 satisfying (3.6), ϕ_1, ϕ_2 say, were found using Newton iteration, thus giving the two required pairs (r_1, ϕ_1), (r_2, ϕ_2), corresponding to two waves, as in the work of Doorly & Smith (1992). However there is a critical value for θ, θ_c say, where the roots coalesce as a double root, i.e. only one wave then gives an algebraic contribution to the integral (2.12) at large times. For values of θ greater than θ_c no roots exist. This critical value for θ thus corresponds to a caustic, or the wingtip of the spot, and occurs when both (3.4) and (3.6) hold and

$$\frac{\partial^2 \psi(r_0, \phi)}{\partial \phi^2} = 0, \tag{3.7}$$

from (3.5), giving

$$2\psi(r_0, \phi_0) \cos^3 \phi_0 = R^2 e^{2r_0} \sin^2 \theta_c. \tag{3.8}$$

Equations (3.4), (3.6), and (3.8) thus provide three equations for r_0, ϕ_0 and the wingtip angle θ_c at any given distance R downstream and consequently govern the overall spot shape.

The spot shape is one of the most intriguing features of the flow solution and it is of interest to consider its development with increasing scaled distance R downstream of the initiation position. At small distances first, i.e. near the spot's trailing edge as $R \to 0$, analysis of (3.4), (3.6), (3.8) is found to yield the following behaviour for r_0, ϕ_0 and θ_c:

$$r_0 = \frac{1}{\sqrt{2}} R + \tfrac{1}{3} R^2 + \ldots, \tag{3.9}$$

$$\phi_0 = \tan^{-1}(\sqrt{2}) + O(R^2), \tag{3.10}$$

$$\theta_c = \sin^{-1}\left(\tfrac{1}{3}\right) - \tfrac{1}{3} R + \ldots. \tag{3.11}$$

The result (3.11) in particular shows, with increasing distance R, the *decrease* of the spread angle away from the trailing edge limit of Doorly & Smith (1992). Again, although the prediction (3.11) of a wedge-like trailing-edge shape only applies strictly for small distances R, it nevertheless provides an estimate close to $R = 1$ of the leading-edge position further downstream at which the wingtip angle θ_c hits zero: see also the next-but-one paragraph.

Second, for the majority of the spot, i.e. at general values of R, $0 < R < 1$, (3.4) and (3.6) were solved numerically, to give the predicted position of the edge of the spot shown in figure 2. It is clear immediately that, as the downstream distance increases, the spread angle of the spot continues to decrease, the long-wave limit of 19.47° in (3.11) holding only at the very rear of the spot. The angle to the point of maximum spot-width is in fact much closer to the experimentally observed value of 11°. Moreover, the overall shape is in encouraging agreement, at least in qualitative terms, with experimental observations of turbulent spots in boundary layers, as given for example by Gad-El-Hak, Blackwelder & Riley (1981).

It seems to be implied also that the wingtip angle θ_c tends to zero at the front of the spot as $R \to 1^-$, as would be expected physically. Equations (3.4), (3.6) and (3.8) may be considered in the limit as $R \to 1$, i.e. $\epsilon \to 0$, where $\epsilon \equiv 1 - R$ denotes the scaled distance from the front. The numerical results appear to show that ϕ_0 also tends to zero at the front and, together with order of magnitude arguments, suggest the following expansions:

$$\phi_0 = \phi_{01} \epsilon^{1/2} L + \ldots, \tag{3.12}$$

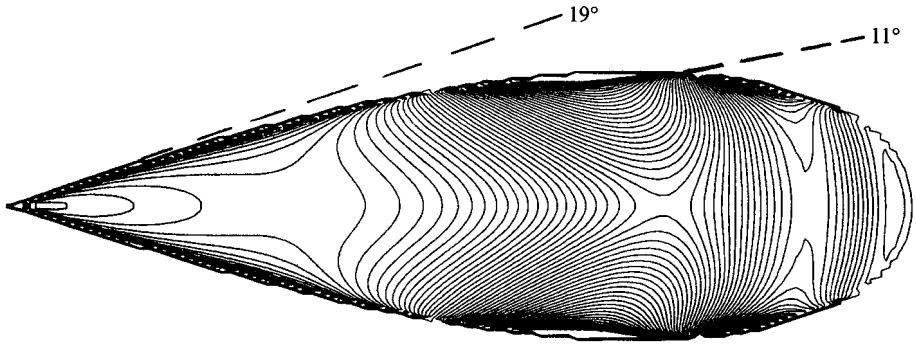

FIGURE 2. The predicted pressure contours at the wall, $y = 0$.

$$\theta_c = \frac{\theta_1 \epsilon^{1/2}}{L} + \ldots, \tag{3.13}$$

where ϕ_{01} and θ_1 are $O(1)$ constants and $L(\epsilon)$ is a relatively slowly varying function of ϵ to be found below. Substitution of (3.12) and (3.13) into (3.4), (3.6), and (3.8) then yields

$$\frac{L^2}{\theta_1^2} e^{-L^2/\theta_1^2} = \epsilon, \tag{3.14}$$

after some working, and hence to leading order $L(\epsilon)$ is determined as

$$L = \theta_1 (\ln(1/\epsilon))^{1/2} + \ldots. \tag{3.15}$$

In consequence the local expansions for r_0, ϕ_0 and θ_c are found to become

$$\theta_c = \frac{\epsilon^{1/2}}{(\ln 1/\epsilon)^{1/2}} - \frac{\epsilon^{1/2} \ln(\ln 1/\epsilon)}{2(\ln 1/\epsilon)^{3/2}} + O\left(\frac{\epsilon^{1/2}}{(\ln 1/\epsilon)^{3/2}}\right), \tag{3.16}$$

$$r_0 = \tfrac{1}{2} \ln(1/\epsilon) - \tfrac{1}{2} \ln(\ln 1/\epsilon) + \ldots, \tag{3.17}$$

$$\phi_0 = \epsilon^{1/2} (\ln 1/\epsilon)^{1/2} + \frac{\epsilon^{1/2} \ln(\ln 1/\epsilon)}{2(\ln 1/\epsilon)^{1/2}} + O\left(\frac{\epsilon^{1/2}}{(\ln 1/\epsilon)^{1/2}}\right). \tag{3.18}$$

The predicted analytical behaviour of θ_c in (3.16) is compared with the numerical results near the front of the spot, in figure 3(*a*,*b*). In figure 3(*a*) the first term only in (3.16) is included, while figure 3(*b*) shows the effect of including the second term. The agreement is felt to be good, given the slow logarithmic convergence of the local expansions in (3.16)–(3.18). The prediction (3.16) confirms that the leading-edge shape of the spot is close to parabolic, although, to be precise, it is slightly sharper than that because of the logarithmic contributions present in (3.16).

4. Numerical results

The complete pressure field may now be calculated as the sum of the contributions from the two waves described in §3. Using the method of stationary phase, the integral in (2.12) may be approximated at large times by

$$\frac{1}{2\pi t} \sum_{i=1,2} e^{i\pi/4(\mathrm{sgn}\psi_{rr}(r_i,\phi_i) + \mathrm{sgn}\psi_{\phi\phi}(r_i,\phi_i))} g(\alpha_i, \beta_i, y) \frac{e^{it\psi(r_i,\phi_i)}}{|\psi_{rr}(r_i,\phi_i)\psi_{\phi\phi}(r_i,\phi_i)|^{1/2}}, \tag{4.1}$$

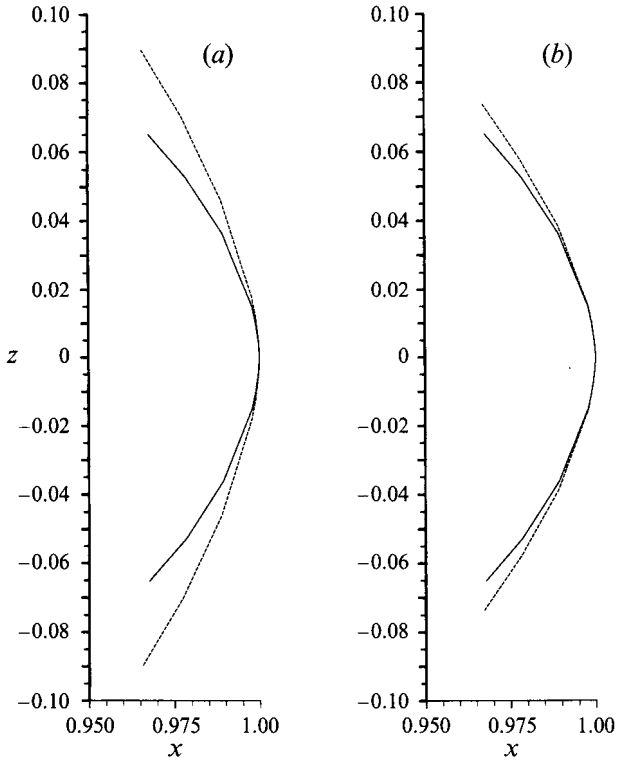

FIGURE 3. The predicted shape of the front: a comparison of the theoretical prediction (dashed) and the numerical result (solid). In (*a*) the first term only in (3.16) is included, in (*b*) the first two terms are used.

where

$$g(\alpha_i, \beta_i, y) = \frac{\hat{Q}(\alpha_i, \beta_i)}{\bar{\alpha}_i \omega}(\hat{\alpha}_i(\omega - \alpha_i y)\cosh \hat{\alpha}_i y + \alpha_i \sinh \hat{\alpha}_i y), \tag{4.2}$$

for the region $0 \leqslant y \leqslant 1$, with a similar expression for the region $y \geqslant 1$. Here $\alpha_i = r_i \cos \phi_i$, and so on.

Figure 2 includes the pressure contours thus calculated, at the wall, $y = 0$, at time $t = 20$, for $\hat{Q} = \mathrm{e}^{-r^2}$. Here comparisons may be made with the experimental measurements of Mautner & Van Atta (1982), for example, suggesting good qualitative agreement. Their results for the wall-pressure signature show a similar division into successive positive and negative pressure regions in the main body of the spot, with the maximum pressure amplitudes occurring at the edges or wingtips.

For a given distance R downstream, as the angle θ decreases from its wingtip value θ_c, the two roots of §3 become distinct, and the phase speed of one wave decreases while that of the other increases. Thus there are two separate though passive critical layers. The group velocities of the two waves are the same, for a given station (x, z), from (3.2), (3.3). Then, as θ becomes small, i.e. near the centreline of the spot, the contribution to the pressure integral from the second root tends to zero, as there the value of $\partial^2 \psi(r_0, \phi)/\partial \phi^2$ at $\phi = \phi_0$ tends to infinity. Consequently there is again only one contributory wave at the centreline, as in two-dimensional theory.

The normal pressure profile of the model spot is shown in figure 4, for the spanwise location $z = 0.0133$ close to the centreline. This view shows that at the rear of

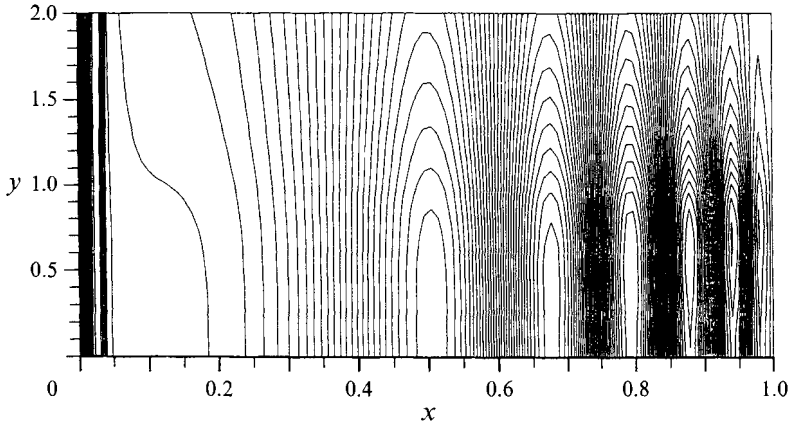

FIGURE 4. Pressure contours at the spanwise location $z = 0.0133$, close to the centreline.

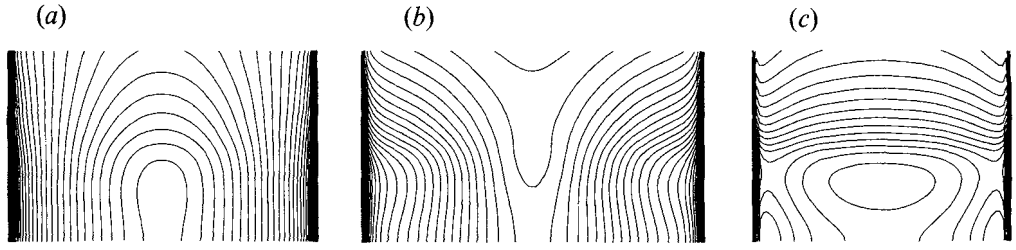

FIGURE 5. Pressure contours for $0 \leqslant y \leqslant 2$ at streamwise locations (*a*) $x = 0.5$, (*b*) $x = 0.7$, (*c*) $x = 0.9$. In (*a*) and (*b*) the pressure is relatively high in the centre and low at the edges. In (*c*) the pressure is relatively high both in the centre and at the edge, and low in between.

the spot the maximum pressure amplitude lies at the wall, but as the downstream coordinate x increases, the maximum leaves the wall and moves steadily out towards the edge of the boundary layer as the contributory waves become ever shorter near the front. This 'lift-up' is again in agreement with the experimental observations, see for example Gad-El-Hak *et al.* (1981).

Figure 5 shows cross-stream sections of the model spot at streamwise distances (*a*) x=0.5, (*b*) x=0.7, (*c*) x=0.9. The maximum pressure amplitude is at the wing tips throughout, where it occurs at the single critical layer $y = \omega/\alpha$. Within the spot, on the other hand, the maximum pressure amplitude occurs at a value of y lying between the two critical layers noted above, and the maximum such y-value, for a given x, occurs along the centreline, giving the spot a central 'bulge'. The lift-up mentioned in the previous paragraph may also be seen by comparing figures 5(*a*)–5(*c*).

5. Further discussion

An investigation of a linear three-dimensional spot disturbance to flow in a model two-dimensional boundary layer is presented above (§§2–4). Despite its simplifications, good agreement is seen (in §4) with experimental observations of some general features of transitional and turbulent spots, at least in qualitative terms. First, the 'arrowhead' shape is predicted, and in keeping with that, second, the theoretical spread angle is reduced by the presence of finite-wavelength modes, which give in the current case a prediction close to 11°. Third and fourth, the 'lift-up' profile and the central

bulge are also in agreement with experimental results and, fifth, the maximum disturbance amplitude occurs at the wingtips both in the model and in observations. Sixth, and more tentative, is the suggestion that the 'calm region' observed in experiments may correspond to the linearly disturbed zone that lags behind the trailing edge of a nonlinear spot (as distinct from the linear trailing edge at the origin, see Figure 1). In fact, from the linear model, figure 2 shows little variation in the pressure anyway in the rear portion of the model spot, while the nonlinear theory predicts that this region remains linear, behind the main nonlinear body of the spot: see Dodia *et al* (1995) and §1 for a more detailed discussion of the calm region. These are all encouraging results and suggest tentatively that the current model may provide some guidelines for further theoretical work on more general linear and nonlinear spot disturbances.

In particular, the analysis of the front or leading edge of the spot, presented in §3, may be extended to other cases. For the case of a spot disturbance in a channel flow, the dispersion relation in the limit $c \to 1^-$, $\bar{\alpha} \to \infty$ (see Smith *et al* 1990) provides a phase function ψ to replace that in §3. Similar analysis of the new function gives a predicted leading edge with a slightly blunter shape than the current model boundary-layer spot, with $z = O(\epsilon^{1/2})$ as $\epsilon \to 0$, i.e. a parabolic shape. Work on other cases is under way, although it might be expected that the parabolic or near-parabolic leading-edge shape is the typical outcome in general.

The model boundary-layer profile assumed in this paper consists of a uniform shear beneath a uniform stream. The model profile may be the most obvious one to take in a first investigation, and clearly it is consistent with triple-deck-like properties for long waves since they depend only on the wall shear and the free-stream speed. It would be of much interest to extend the analysis to linear and nonlinear waves for other profiles, e.g. small linear or nonlinear disturbances to straight-line profiles, or small nonlinear disturbances to smooth profiles, as mentioned in §1, but it is equally interesting to consider the influences of the underlying basic pressure gradient according to the current model. From §2 the speed of the stream is $\lambda\delta$, where δ is the displacement thickness and λ the skin friction. The three velocity components are nondimensionalized on this speed and the three length coordinates on δ, as mentioned in §1. Thus it is possible to examine the effects of varying the displacement thickness and the shear. If, for example, the displacement thickness is increased by an adverse pressure gradient, with the free-stream speed remaining fixed or decreased, the skin friction λ may decrease as expected. The disturbance development lengthscale then increases, because of the scaling on δ mentioned above, and the timescale for the disturbance ($\propto \lambda^{-1}$) increases due to the decrease in λ. This would seem to imply that the spot would tend to have a larger size and perhaps last for a greater distance and a longer time, under the influence of an adverse pressure gradient. The implication would seem to be sensible physically, granted that viscous sublayer bursting would also tend to be enhanced.

The large-time analysis presented in §3 considers the behaviour of the disturbance over large lengthscales, with x, z of $O(t)$ and with $O(1)$ wavenumbers, α, β, covering the majority of the spot. Near the trailing edge of the spot on the other hand the alternative scalings $x, z = O(t^{1/2})$, $\alpha, \beta = O(t^{-1/2})$ apply, as in Doorly & Smith (1992) and Smith *et al.* (1994), yielding a region of elliptic properties. Similarly near the front, where the coordinate x is close to t, corresponding to disturbances travelling at almost the free-stream speed of unity, the short-wave developments over a much shorter scale have still to be considered. There the initial disturbance shape could become more important in the large-time analysis, via the function $\hat{Q}(\alpha, \beta)$ in the integrals in equation (2.12). In addition, the comparatively thin region at the spot

wingtips, in which an Airy function acts locally to reduce the disturbance amplitude to zero exponentially outside the spot may also play a significant role in a tiny zone right at the leading edge.

It is shown in §4 that the maximum disturbance amplitude moves towards the edge of the boundary layer, $y = 1$ in the present model, near the front of the spot: see also 'lift-up' at the start of this section. The frontal region described in the previous paragraph is thus situated near $y = 1$. Analysis of this region may be instructive when considering more general spot disturbances, whether linear or nonlinear, including an examination of the decay of the disturbance as y decreases away from $y = 1$. Other issues that merit further study include the generalizations of the trailing-edge shape prediction in (3.11) in §3, and especially the sign of the second term there, the leading-edge shape prediction also in §3 and earlier in this section, the overall spread angle, currently near 11°, and the interplay between nonlinear interactions and short-scale effects. These nonlinear effects could take the form of resonant-triad interactions of the waves discussed here, see, for example, Craik (1971).

Altogether, the present simple inviscid model appears to agree remarkably well with experiments, as described at the beginning of this section. The importance of its findings should not be exaggerated of course and may be fortuitous but, against that, it could be concluded that relatively simple considerations concerning short-scale effects as here, allied with the influence of nonlinearity in the middle of the spot (Dodia *et al.* 1995), combine to control the overall spot development in practice. Again, there seem to be few if any other linear or nonlinear studies of initial-value problems which are not restricted to narrow-band disturbances. The current study addresses a *wide* band. In particular Tollmien–Schlichting contributions (see, for example, Ryzhov & Savenkov 1987; Smith 1986), which are narrow-band, are left comparatively far behind the major portions of the spot, being confined near the origin in figures 2, 4 and being irrelevant to the real spot characteristics at large times. Similar considerations apply to other initial conditions such as those initiating weakly nonlinear vortex–wave interactions (Smith, Brown & Brown 1993) or unsteady critical layers (Goldstein & Hultgren 1988), which are again narrow-band in nature and hence have little impact in the current regime or for real spots. At low amplitudes for laminar spots there are at least three factors all tending to limit the spot spreading rate, namely compressibility Doorly & Smith (1992), viscosity (Gaster 1975; Gaster & Grant 1975) and short-scale inviscid effects as in the present study. At higher amplitudes however it is felt likely that the spreading rate is controlled mostly by the short-scale effects above combined with nonlinearity as in Smith *et al.* (1994), and with compressibility if present, at least until the amplitudes are sufficiently large as to provoke the viscous sublayer eruptions discussed in the last-named reference. The reduction of the theoretical spread angle from 19.47° to approximately 11° is certainly an encouraging feature.

It is worth remarking that the same 19.47° angle is found for ship wakes (Lighthill 1978) and for rotating fluids Cheng & Johnson (1982), while a corresponding independent analysis for channel flows is given by Widnall (1984). Reduction of the angle by short-scale effects could occur in these contexts and there may be applications of those effects and others studied herein also in a variety of different flows.

Thanks are due to EPSRC for support for RGAB and for computational facilities, to Dr A. J. Grass for many interesting discussions and to the referees for their comments.

REFERENCES

CHENG, H. K. & JOHNSON, E. R. 1982 Inertial waves above an obstacle in an unbounded rapidly rotating fluid. *Proc. R. Soc. Lond.* A**383**, 71.

CRAIK, A. D. D. 1971 Nonlinear resonant instability in boundary layers. *J. Fluid Mech.* **50**, 393.

DODIA, B. T., BOWLES, R. G. A. & SMITH, F. T. 1995 On effects of increasing amplitudes in a boundary-layer spot. *J. Engng Maths* (submitted).

DOORLY, D. J. & SMITH, F. T. 1992 Initial-value problems for spot disturbances in incompressible or compressible boundary layers. *J. Engng Maths* **26**, 87.

ELDER, J. W. 1960 An experimental investigation of turbulent spots and breakdown to turbulence. *J. Fluid Mech.* **9**, 235.

EMMONS, H. W. 1951 The laminar-turbulent transition in a boundary layer, Part 1. *J. Aero. Sci.* **18**, 490.

GAD-EL-HAK, M., BLACKWELDER, R. F. & RILEY, J. J. 1981 On the growth of turbulent regions in laminar boundary layers. *J. Fluid Mech.* **110**, 73.

GASTER, M. 1968 The development of three-dimensional wave-packets in a boundary layer. *J. Fluid Mech.* **32**, 173.

GASTER, M. 1975 A theoretical model of a wave-packet in the boundary layer on a flat plate. *Proc. R. Soc. Lond.* A**347**, 271.

GASTER, M. & GRANT, I. 1975 An experimental investigation of the formation and development of a wave-packet in a laminar boundary layer. *Proc. R. Soc. Lond.* A**347**, 253.

GLEZER, A., KATZ, Y. & WYGNANSKI, I. 1989 On the breakdown of the wave-packet trailing a turbulent spot in a laminar boundary layer. *J. Fluid Mech.* **198**, 1.

GOLDSTEIN, M. E. & HULTGREN, L. S. 1988 Nonlinear spatial evolution of an externally excited instability wave in a free shear layer. *J. Fluid Mech.* **197**, 295.

HENNINGSON, D., LUNDBLADH, A. & JOHANSSON, A. V. 1993 A mechanism for by-pass transition from localized disturbances in wall-bounded shear flows. *J. Fluid Mech.* **250**, 169.

KACHANOV, Y. S., RYZHOV, O. S. & SMITH, F. T. 1993 Formation of solitons in transitional boundary layers: theory and experiment. *J. Fluid Mech.* **251**, 273.

KATZ, Y., SEIFERT, A. & WYGNANSKI, I. 1990 On the evolution of the turbulent spot in a laminar boundary layer with a favourable pressure gradient. *J. Fluid Mech.* **221**, 1.

LIGHTHILL, M. J. 1978 Ship waves. In *Waves In Fluids* (ch. 3.10). Cambridge University Press.

MAUTNER, T. S. & VAN ATTA, C. W. 1982 An experimental study of the wall-pressure field associated with a turbulent spot in a boundary layer. *J. Fluid Mech.* **118**, 59.

RYZHOV, O. S. & SAVENKOV, V. I. 1987 Asymptotic theory of a wave packet in a boundary layer on a plate. *Prikl. Matem. Mekhan.* **50**, 820.

SMITH, F. T. 1986 Steady and unsteady 3D interactive boundary layers. *Computers Fluids* **20**, 293.

SMITH, F. T. 1992 On nonlinear effects near the wingtips of an evolving boundary-layer spot. *Phil. Trans. R. Soc. Lond.* A**340**, 131.

SMITH, F. T., BROWN, S. N. & BROWN, P. G. 1993 Initiation of three-dimensional nonlinear transition paths from an inflectional profile. *Eur. J. Mech.* **12**, 447.

SMITH, F. T. & BURGGRAF, O. R. 1985 On the development of large-sized short-scaled disturbances in boundary layers. *Proc. R. Soc. Lond.* A**399**, 25.

SMITH, F. T., DODIA, B. T. & BOWLES, R. G. A. 1994 On global and internal dynamics of spots: a theoretical approach. *J. Engng Maths* **28**, 73.

SMITH, F. T., DOORLY, D. J. & ROTHMAYER, A. P. 1990 On displacement thickness, wall-layer and mid-flow scales in turbulent boundary layers and slugs of vorticity in pipes and channels. *Proc. R. Soc. Lond.* A**428**, 255.

WIDNALL, S. E. 1984 Growth of turbulent spot in plane Poiseuille flow. In *Turbulence and Chaotic Phenomena in Fluids* (ed. T. Tatsumi), p. 93. Elsevier.